DEPARTMENT OF CHEMISTRY, UNIVERSITY OF JYVÄSKYLÄ
RESEARCH REPORT No. 64

EXPERIMENTAL AND THEORETICAL STUDIES ON SOME QUINONE AND QUINOL RADICALS

BY

JUSSI ELORANTA

Academic Dissertation
for the Degree of
Doctor of Philosophy

Jyväskylä, Finland 1997
ISBN 951-39-0090-8
ISSN 0357-346X

RESEARCH REPORT No. 64

EXPERIMENTAL AND THEORETICAL STUDIES ON SOME QUINONE AND QUINOL RADICALS

BY

JUSSI ELORANTA

Academic Dissertation
for the Degree of
Doctor of Philosophy

To be presented, by permission of the Faculty of Mathematics and Natural Sciences of the University of Jyväskylä, for public examination in Auditorium S-212 of the University on Nov 28th, 1997, at 12 o'clock noon

University of Jyväskylä,
Jyväskylä, Finland
ISBN 951-39-0090-8
ISSN 0357-346X

URN:ISBN:978-952-86-0130-2
ISBN 978-952-86-0130-2 (PDF)
ISSN 0357-346X

University of Jyväskylä, 2024

CONTENTS

ACKNOWLEDGMENTS

I wish to thank the following people for help and support during this work: Jorma Eloranta, Tamara Eloranta, Tuija Heinonen, Mikko Vuolle, Jari Eloranta, Reijo Mäkelä, Virpi Vatanen, Antti Grönroos, Hilkka Heikkilä, Kari Vaskonen, Reijo Suontamo, Erkki Kolehmainen, Reijo Kauppinen, Tapani Sorsa, Erkki Järvinen, Marcus Karmalahti, Sisko Siikamäki, and Juha Linnanto. Financial support by Ella ja Georg Ehrnroothin Säätiö is gratefully acknowledged.

Jyväskylä, Nov 1997

Jussi Eloranta

LIST OF ORIGINAL PUBLICATIONS

This thesis is based on the following publications:

1. Eloranta, J. M., Vatanen, V., Grönroos, A., Vuolle, M., Mäkelä, R., Heikkilä, H., Comparison of Spin Density Calculation Methods for Various Alkyl-Substituted 9,10-Anthraquinone Anion Radicals in the Solution Phase. (1996) *Magn. Reson. Chem.* **34**, 898-902.

https://doi.org/10.1002/(SICI)1097-458X(199802)36:2<98::AID-O MR228>3.0.CO;2-Q

2. Eloranta, J. M., Vatanen, V., Grönroos, A., Vuolle, M., Mäkelä, R., Heikkilä, H., EPR, ENDOR and TRIPLE Resonance of Amino-Substituted 9,10-Anthraquinone Radicals and the Rotation of the Amino Groups in the Solution Phase. (1996) *Magn. Reson. Chem.* **34**, 903-907.

https://doi.org/10.1002/(SICI)1097-458X(199611)34:11<903::AID-O MR986>3.0.CO;2-8

3. Eloranta, J. M., Vatanen, V., Vaskonen, K., Suontamo, R., Vuolle, M., Molecular Orbital Study of Conformational Isomers and Rotational Barriers of Methyl Substituted Hydroquinone Cation Radicals. (1997) *J. Mol. Struct. (Theochem)*, in press.

https://doi.org/10.1016/S0166-1280(97)00152-8

4. Eloranta, J. M., Suontamo, R., Vuolle, M., Molecular Orbital Study of the Isotropic Hyperfine Coupling Constants of Hydroquinone and Tetramethylhydroquinone Cation Radicals. (1997) *J. Chem. Soc., Faraday Trans.* **93**, 3313-3317 (1997).

https://doi.org/10.1039/A701894K

5. Eloranta, J. M., Vuolle, M., Temperature Dependence of the Isotropic Hyperfine Coupling Constants in 1,4-hydroquinone and 1,4-dihydroxy-naphthalene Cation Radicals. (1997) *Magn. Reson. Chem.*, in press.

https://doi.org/10.1002/(SICI)1097-458X(199802)36:2<98::AID-O MR228>3.0.CO;2-Q

1. PREFACE

Radical molecules are usually very reactive and they play an important role in many reaction mechanisms as intermediates. For this reason it is important to gain information about these reactive species. Electron magnetic resonance (EMR) spectroscopy provides an important experimental method for studying the magnetic properties and dynamics of the radical molecules.

Quinones represent a class of biologically important compounds which usually are good electron acceptors and in some cases also electron donors. Both processes result in a radical molecule which can be studied by EMR spectroscopy. In the present work the properties of alkyl- and amino-substituted 9,10-anthraquinone anion radicals, as well as hydroquinone and 1,4-dihydroxynaphthalene cation radicals were explored with experimental and theoretical methods. The dynamic processes encountered in these compounds in the liquid phase provide an interesting and challenging research field in which this study provides new information about the rotation barrier heights and the temperature dependences of the isotropic hyperfine coupling constants. The static magnetic properties were also obtained to provide reference data for these compounds.

2. OVERVIEW OF ELECTRON MAGNETIC RESONANCE

Electron paramagnetic resonance spectroscopy (EPR) may be regarded as an extension of the famous Stern-Gerlach experiment.[1,2,3] In the 1920s Stern and Gerlach showed that an electron magnetic moment in an atom can only take discrete orientations in the presence of an external magnetic field. Later Breit and Rabi derived the resultant energy levels of a hydrogen atom in a magnetic field where one has additional angular momentum arising from the proton.[4] Rabi further studied the transitions between the levels by using an oscillating magnetic field.[5] A few years later Zavoisky performed the first EPR experiment by detecting a radio frequency absorption from a $CuCl_2 \cdot 2H_2O$ sample in a magnetic field.[6] Later experiments were extended to higher frequencies, namely the microwave region. Nowadays, the usual frequency of a modern EPR spectrometer is *ca.* 9 GHz.

The theoretical and experimental methods of electron magnetic resonance relevant to this work will be reviewed here briefly.

2.1 EPR spectroscopy

The EPR spectrum is recorded by varying the magnetic field strength and monitoring the absorption of the applied electromagnetic radiation by the sample. The reason for varying the strength of the magnetic field instead of the frequency of electromagnetic radiation is purely technical. Due to the modulation scheme used by most EPR spectrometers the spectrum is displayed as the first derivative of the absorption spectrum. This modulation scheme enhances the sensitivity of the spectrometer remarkably. EPR spectrometers are usually classified by the frequency of the electromagnetic radiation used: X-band (6 - 11 GHz), K-band (11 - 36 GHz), Q-band (36 - 46 GHz), and W-band (56 - 100 GHz).

The spin energy levels of organic π-radicals in the liquid phase are approximately given by:

(1) $$E(m_S,m_{I_1},...,m_{I_n}) = g\beta Bm_S + hm_S\sum_{i=1}^{n} A_i m_{I_i}$$

where g is the g-value of the unpaired electron (characteristic for the radical), β is the Bohr magneton, B is the magnitude of the external magnetic field, m_S is the quantum number of the unpaired electron, h is Planck's constant, A_i is the isotropic hyperfine coupling constant (IHFC; Hz), and the m_{I_i}'s are the nuclear spin quantum numbers.[7] The effects of spin-orbit coupling in eqn. (1) have been embedded into variable g. For organic π-radicals the spin-orbit coupling is usually small and the g-value is then close to the g-value of a free electron.[7] For all radicals studied in this work the observed g-values were within a range of 2.0032 - 2.0050.

The allowed transitions in the EPR spectroscopy to the first order are $\Delta m_S = \pm 1$ and $\Delta m_I = 0$. In the EPR experiment the allowed transitions among the energy levels of eqn. (1) are induced by electromagnetic radiation in the presence of an external magnetic field. The energy corresponding to the electromagnetic radiation is given by $h\upsilon$, where υ is the frequency of the electromagnetic radiation (Hz). In order to observe a hyperfine coupling between the unpaired electron and the nucleus, this nucleus must have a nonzero magnetic moment.

The relative intensities of the EPR transitions are affected by the statistical distribution of nuclear states. For example, two magnetically equivalent nuclei of nuclear spin 1/2 give rise to nuclear spin states (α,α), (β,α), (α,β), and (β,β). The second and third states correspond to degenerate transitions; therefore the intensity of this transition is twice as great as that of the first and the last transitions (1:2:1). In the case of nuclear spin 1/2 the intensities are given by the coefficients of the binomial expansion. For higher nuclear spins a modified binomial expansion must be used.[7]

The macroscopic behavior of the unpaired electron spins may be described by the Bloch equations.[7,8,9] The rotating frame solution of the Bloch equations result in the following lineshape function for EPR absorption:

$$I(\omega) \propto \frac{B_1 T_2}{1+T_2^2(\omega_0-\omega)^2+\gamma_e^2 B_1^2 T_1 T_2} \qquad (2)$$

where B_1 is the amplitude of the electromagnetic radiation, T_2 is the spin-spin relaxation time, ω_0 is the unpaired electron Larmour frequency, ω is the frequency of the electromagnetic radiation, γ_e is the free-electron magnetogyric ratio, and T_1 is the spin-lattice relaxation time.[7,8] If the last term in the divisor of eqn. (2) is large then the intensity of the absorption is small. Since organic radicals usually have rather long spin-lattice relaxation times in the liquid phase, a low microwave power must be applied in order to avoid power saturation.[8] The typical microwave power applied in this work was in the range of 0.1 - 0.5 mW.

The Bloch equations may be modified to include other relaxation effects, such as molecular exchange.[9,10] An alternative and more elegant method based on density matrix formalism may be used to describe the dynamic effects on the EPR spectrum. The density matrix obeys its equation of motion (Liouville equation).[8] The diagonal elements of the density matrix ρ represent the fractional populations of the corresponding states and the non-diagonal elements describe the coupling of the corresponding states by the Hamiltonian.

The density matrix formalism may be used to obtain lineshape functions in the case of two special phenomena which are important in liquid phase EPR studies; namely, the alternating linewidth effect caused by chemical exchange and the nuclear spin dependent line broadening caused by introduction of anisotropic effects into the spectrum. The latter effect is usually observable in the low temperature region where the viscosity of the solvent is high. These two cases have been implemented in the xemr program developed during this work.[11]

In the case of intramolecular exchange we assume that the nuclear spin states of the molecules do not change during the process. This is certainly true when a radical molecule is transformed from one isomer to another. In this case the following result for the lineshape may be derived from the steady state solution of the Liouville equation and further by calculation of the expectation value of the unpaired electron spin rising operator:

$$f(\omega) = \mathrm{Im}\left(\frac{-iC\sum_{k=1}^{N_c} F_k(\omega)}{1+\frac{1}{\tau}\sum_{k=1}^{N_c} F_k(\omega)}\right), \qquad (3)$$

$$F_k(\omega) = \frac{n_k}{i(\omega-\omega_{0,k})-\frac{1}{T_2^k}-\frac{1}{\tau}}$$

where N_c is the number of conformations, n_k is the fractional population of the structure containing the kth line ($1/N_c$), $\omega_{0,k}$ is the Larmour frequency of kth line, T_2^k is the spin-spin relaxation time of kth line, and τ is the average life time of all occurring species.[12] The lines contained in the sum of eqn. (3) all have the same nuclear spin quantum numbers occurring in the different structures. The total spectrum is then obtained by summing over the lines originating from all the nuclear spin quantum number combinations. The lines having the same positions in all structures stay sharp and the "moving" lines broaden. The broadening effects start to show up in the spectrum when the exchange rate is of the same order as the IHFC (in Hz). The average first order rate constant k for the isomerization reaction can be obtained from the inverse of $N_c\tau$. The eqn. (3) is a simple and fast method for calculating the exchange broadened spectra. A more comprehensive and complicated method, where the rate constants for conversion between each structure may be obtained, has been described by Heinzer.[13] Both the Norris and the Heinzer methods have been implemented in the xemr program.[11] For an example of this linewidth alternation phenomenon, see paper 5 / Fig. 2.

Further, the energy of activation may be obtained from the well-known Arrhenius plot (ln k vs. 1/T). By way of an example an Arrhenius plot of the hydroxyl group rotation in the hydroquinone cation radical measured in this work is shown in Fig. 1. The rate constants were obtained directly from the xemr optimization runs.

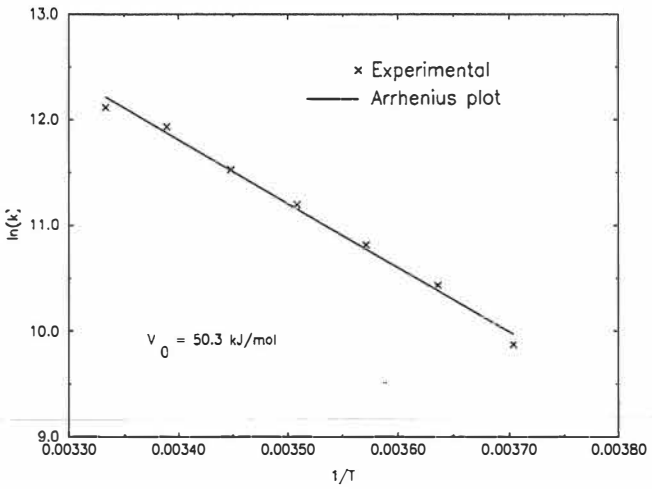

Fig. 1. Arrhenius plot of the hydroxyl group rotation in the hydroquinone cation radical. The radical was generated in a mixture of sulfuryl chloride fluoride and fluorosulfonic acid. V_0 indicates the energy of activation obtained by the least squares fitting. The temperature range of 270 - 300 K is shown.

The anisotropic line broadening can be modelled with the Redfield equation, which is an approximate derivation of the density matrix equation. It can be shown that the resulting linewidth is of the form:

(4) $$\frac{1}{T_2} = A + \sum_i B_i m_{I_i} + \sum_i C_i m_{I_i}^2 + \sum_{i<j} D_{ij} m_{I_i} m_{I_j}$$

where parameter A depends on the interaction of traceless anisotropic g and hyperfine coupling matrices with themselves as well as other line broadening mechanisms; B is the cross interaction term of traceless anisotropic g and hyperfine couplings; C is the interaction of

traceless anisotropic hyperfine coupling with itself, and *D* corresponds to the interaction between traceless anisotropic hyperfine couplings of different groups of completely equivalent nuclei.[7,8] Basically, these constants depend on the liquid phase rotation correlation time of the radical and the tensor inner products of the traceless anisotropic g and hyperfine coupling matrices. When degenerate EPR transitions are present, it is important to distinguish the difference between symmetrically equivalent and completely equivalent groups of nuclei. Complete equivalency means that the nuclei have the same static and time dependent Hamiltonians. In the symmetric case only the time averaged Hamiltonians for the nuclei are same.[8] The effect of eqn. (4) can clearly be seen as broadened high field lines in the low temperature region for the studied quinone samples as shown in Fig. 2. It should be remembered that the Redfield theory is valid only for rotation correlation times 10^{-9} s or shorter at X-band frequencies.[8]

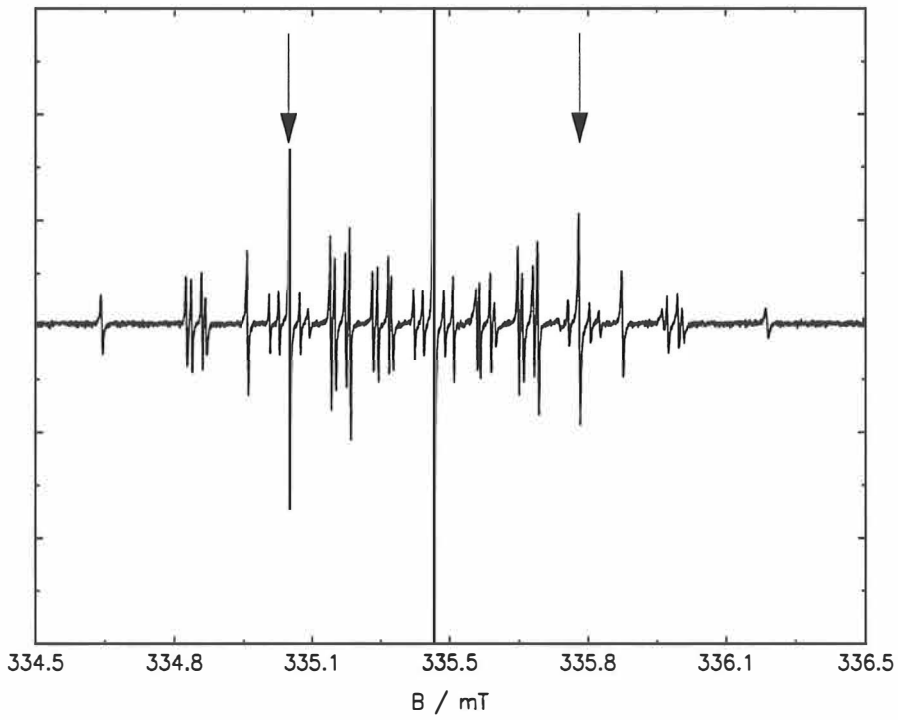

Fig. 2. Experimental EPR spectrum of hydroquinone cation radical in a mixture of sulfuryl chloride fluoride and fluorosulfonic acid at 200 K. The spectrum consists of two overlapping species, the cis and trans forms.

2.2 ENDOR spectroscopy

In the liquid phase ENDOR experiment a peak from the EPR spectrum is first selected for monitoring and the selected position is maintained accurately by using a field/frequency lock. Then the EPR signal is power saturated so that its intensity is reduced. In this work the applied saturating microwave power levels were in range of 10 - 30 mW. A second electromagnetic radiation, usually called the NMR radiation, is chosen orthogonal to the external magnetic field and the EPR radiation. By applying NMR radiation of the nuclear transition frequency to the sample the corresponding spin energy levels become coupled. If the relaxation conditions are favorable, the EPR signal is restored. An ENDOR spectrum consists of the changes in EPR signal intensity when the NMR field is swept over the measurement interval. A group of equivalent nuclei produce a peak pair centered around the nuclear ENDOR frequency (ν_n; Hz). The peaks are separated by the absolute value of IHFC (A; Hz). Alternatively, if $|A|/2 > \nu_n$ then the peak pair is centered at $|A|/2$ and separated by $2\nu_n$. The nuclear ENDOR frequency depends on the magnitude of the external magnetic field and the nuclear magnetic moment.

The selection rule for an ENDOR transition is $\Delta m_I = \pm 1$ and therefore the nuclear Zeeman-energy contribution must be added to eqn. (1). The possibility to obtain an ENDOR spectrum depends on the relaxation times between energy levels: electron spin relaxation T_1, nuclear spin relaxation T_{1n}, and cross relaxations T_{x1} and T_{x2}.[14,15] Because the line intensities depend heavily on the relaxation parameters the number of nuclei contributing to the same hyperfine transition cannot usually be determined from the ENDOR spectrum. When cross relaxations are ignored, it can be shown that the solvent viscosity and sample temperature may be adjusted to obtain the best ENDOR signal.[15] For the molecules and solvents studied in this work, the best ENDOR enhancements were usually obtained near the freezing points of the solvents. The sign of the hyperfine coupling changes the order of the

energy levels but leaves the overall spectrum unaltered.[14] The ENDOR intensities are typically from one to ten percent of the EPR signal intensities and therefore the samples must have rather high radical concentrations (*ca.* 5 mmol dm^{-3}).

The liquid phase ENDOR experiments are usually more difficult to perform than those in the solid phase because the electron spin relaxation is much faster in the liquid phase. The nuclear transitions have to be driven at a rate comparable to the electron spin relaxation, which means that higher amplitude NMR radiation must be used. The applied NMR radiation power in this work was in the range of 300 - 500 W. An example of a liquid phase ENDOR spectrum can be seen in paper 1 / Fig. 3. This ENDOR spectrum consists of three groups of equivalent protons. In this case the molecular symmetry suggests that there should be four groups of equivalent protons but two of these groups have accidental equivalency. Here the proton ENDOR frequency was *ca.* 14 MHz at 340 mT.

2.3 TRIPLE general spectroscopy

TRIPLE general spectroscopy is closely related to the ENDOR spectroscopy. In contrast to the ENDOR experiment the TRIPLE general experiment has one extra NMR radiation oriented in such a way that it is perpendicular to all the other fields. One of the NMR radiations is "pumping" some selected ENDOR transition while the frequency of the other NMR radiation is swept over the measurement interval. The first NMR radiation short-circuits the given nuclear relaxation path affecting the intensities of all ENDOR peaks. The TRIPLE general spectrum may be used to obtain the relative signs of the IHFCs by inspecting the intensity changes of the other ENDOR peak pairs.[15] An example of a TRIPLE general spectrum is shown in Fig. 3. Here the spectrum gives a hint of the ethyl proton IHFC because very often the ring protons and, the methyl and ethyl protons have the opposite signs. This interpretation appears to be in agreement with the theoretical calculations (see paper 1).

It should be noted that the ENDOR peak intensity behavior depends on the sign of the nuclear g_N value, and thus this has to be taken into account for such nuclei.[15]

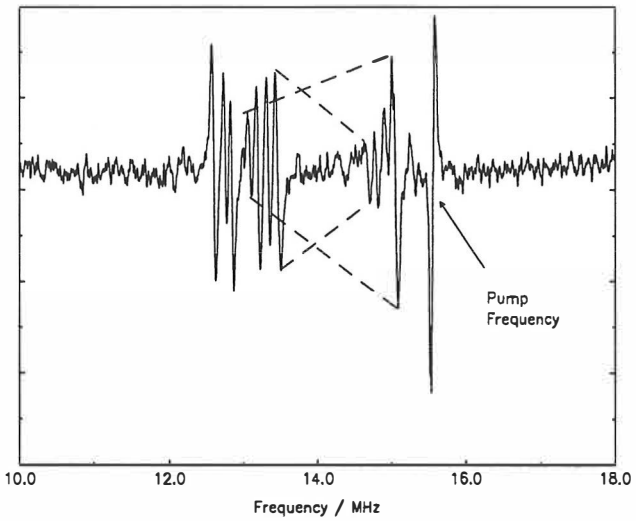

Fig. 3. An example TRIPLE general spectrum of the 2-ethyl-9,10-anthraquinone anion radical is presented. The spectrum shows that one of the IHFCs has a different sign compared to the other IHFCs.

2.4 Simulation of isotropic EPR spectra

The isotropic EPR spectrum can be simulated provided that the spectral parameters are known. Among these parameters are the IHFCs, linewidth, signal intensity, parameters of eqns. (3) and (4), and other parameters. In the first order EPR spectrum simulation, the transitions between the energy levels of eqn. (1) and the statistical appearance of the nuclear states are generated. Usually the simulation procedure first generates the stick spectrum, which is then convoluted with the lineshape function. This can sometimes be done in an effective way by the transformation to the corresponding Fourier space, where the convolution is just a multiplication operation. This method cannot, however, be applied when the lines have varying widths. If the simulation contains many species, the spectra are summed to obtain the total spectrum. Once the spectrum has been simulated, it can be compared to

the experimental EPR spectrum by calculating the root-mean-square (RMS) difference between the spectra. The RMS value gives correctness criteria for the simulation. The process can easily be automated by minimizing the RMS value respective to the spectral parameters. The minimization problem is a global minimization problem which usually embraces of many closely located local minima. For this reason the otherwise effective gradient based methods cannot be applied since they easily get trapped in local minima. Typical minimization methods applied are, for example, the Monte Carlo (MC) and simplex methods.[16,17,18]

The MC method is a heavily random method, where the trial points are chosen by random and, if the RMS of a trial point is better than the current one, then the trial point is chosen as the current point. This process is typically repeated a few thousand cycles. The initial guess and a maximum change limit for each variable are given before the optimization is started. This restricts the random search to the region where the solution is expected to be. A good initial guess for IHFCs is generated by the ENDOR measurements, where the number of equivalent nuclear groups are unknown but can usually be guessed on the basis of the molecular symmetry. A general rule is that as many parameters as possible should be obtained by hand and kept constant during the optimization. The choice of a maximum change limit of the parameters is two-fold: if chosen too small the process gets trapped into local minima easily, and if chosen too large the process converges to the minimum very slowly.

In the simplex method a simplex of n+1 corner points, where n is the number of variables in the optimization problem, is generated in the optimization space. The initial simplex points are chosen by random and are limited by the maximum change limit parameter as described above. Then at each simplex iteration the point having the worst RMS value is discarded and a new point is chosen. The new point is selected from the opposite side of the simplex where the worst point was located. Various heuristics may be applied to scale the length of this step and thereby enhance the convergence speed. For exact details, see Ref. 11. It was observed during this work that at least a few hundred cycles of the MC method

should be applied before the simplex method which will then locate the minimum more effectively.

Some general rules should be applied when performing simulation fitting with the xemr program.[11] For example, the linewidth can best be obtained from the central peak (if it exists) when the anisotropic broadening is present, because the central line has all the nuclear quantum numbers zero (cf. eqn. (4)). This peak also provides a good way of judging the correctness of the intensity variable of the simulation. Many local minima usually exist in the direction of the intensity variable. The maximum change limits should first be chosen "large", and when the simulation process proceeds, then the limits may be narrowed. Sometimes restrictions among the optimizable parameters must be issued in order to obtain meaningful results. For example, the simulation of the cis and trans forms of the hydroquinone cation is greatly simplified when the hydroxyl proton IHFC and positions of the first peaks are forced to be the same for both the species. This applies especially to the intramolecular exchange simulation of the hydroquinone cation, which consists of four different species.

The application of special non-linear least squares optimization procedures should further increase the convergence speed near the minimum. The implementation of these methods to xemr are in progress.

3. EXPERIMENTAL

Preparation of the quinone radicals usually requires high vacuum conditions, because the radicals react easily with triplet state oxygen molecules and the oxygen also causes unwanted line broadening of the EPR spectrum. Therefore the samples studied in this work were prepared in vacuum cuvettes (*ca.* 10^{-7} Torr), in special cuvettes from which the oxygen was removed by flushing nitrogen through the cuvette, or in closed argon gas driven loop-flow cuvettes. Sketches of the vacuum cuvette and closed loop-flow cuvette used in this work are shown in Figs. 4 and 5.

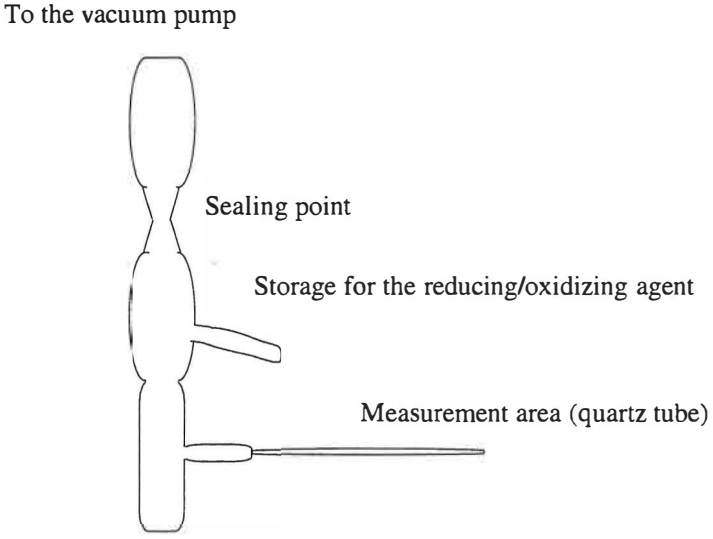

Fig. 4. Sketch of the EPR vacuum cuvette. The base of the cuvette is pyrex glass.

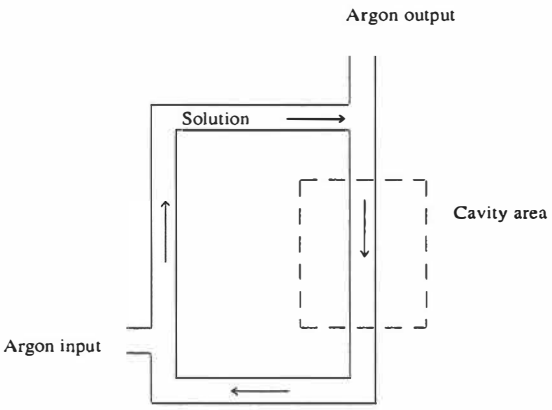

Fig. 5. Sketch of the closed loop-flow cuvette driven by argon gas. The amount of required compounds can be easily adjusted to obtain the best measurement conditions or to perform series of concentration dependent measurements.[19,20,21]

In the case of vacuum samples the chemicals required for the sample were first inserted into the cuvette, then the sample was frozen in liquid nitrogen, and the cuvette was sealed by flame after two or three pump-freeze-thaw cycles. For some samples UV irradiation was required for radical generation. It is important not to produce a too high radical concentration, because the Heisenberg exchange effect will cause considerable line broadening (max. 10^{-4} mol dm^{-3}).[8]

3.1 Anion radicals of alkyl- and amino-substituted 9,10-anthraquinones

The alkyl- and amino-substituted 9,10-anthraquinones exist in the non-protonated quinone -forms at pH higher than *ca.* 9.[22] High pH should be used when producing the anion radicals of these compounds, because otherwise a mixture of some half protonated forms may be the result. Also, the proton exchange with the solvent could cause considerable line broadening effects. Both alkyl- and amino-substituted 9,10-anthraquinones are soluble in alcohol-water mixtures. Ethanol-water combinations usually yield good results. In some cases dimehylformamide or dimethylsulfoxide could also be used as solvents. For some

compounds the high alkaline concentration alone is sufficient to produce high enough radical concentrations for measurements. If this is not the case, then sodium dithionite or glucose may used as a reducing agent. Exact details of the methods for producing the anion radicals of these compounds are given in papers 1 and 2. The high alkaline concentrations can cause unwanted side reactions, especially with substituents at β-positions of the anthraquinone ring. Therefore optimal adjustment of the pH is very important. If UV irradiation is required for radical generation then special care must be taken not to introduce any side reactions. The outlined methods produce high enough radical concentrations for measurement of EPR, ENDOR, and TRIPLE general spectra.

The anion radicals were also produced in liquid ammonia or dimethoxyethane by the alkali metal reduction, but these methods are more laborious than the methods presented above.

3.2 Cation radicals of hydroquinone and 1,4-dihydroxynaphthalene

The hydroquinone and 1,4-dihydroxynaphthalene cation radicals may be produced under high vacuum conditions with strong acids as oxidants. The parent compound, in both cases, may be the quinone or the quinol form, which both result in the same quinol cation radical. Usually fumic sulfuric acid or fluorosulfonic acid is used as an oxidant with a suitable solvent. These acids, however, cause some slow side reactions which presumably involve substitution of the hydroxyl group. Therefore the samples must be measured on the same day as they are prepared. In this work nitromethane (NM) and sulfuryl chloride fluoride (SCF) were used as solvents. The advantage of using SCF instead of NM is the larger temperature scale, that is *ca.* 150 - 300 K vs. 200 - 300 K. The acid concentration needs to be kept to a minimum in order to obtain the best resolution for the EPR spectra. It was observed that SCF and sulfuric acid cannot be used together since they result in two phases. This means that the deuterated sulfuric acid cannot be used for the deuteration of the hydroxyl group protons in this solvent. See paper 5 for exact details on sample preparation.

For more detailed information on the suitable solvents and reducing/oxidizing agents for quinones and quinols, see Ref. 23. The special cuvette used in this work is also documented in Ref. 23.

4. COMPUTATIONAL BACKGROUND

The rapid development of powerful computers has made computational chemistry available as a useful tool for interpreting experimental results and sometimes for giving a prediction of what is to be expected in an experiment.

A short introduction to the applied computational methods used in this work will be given below. A good recent review of the electronic structure methods was given by Head-Gordon.[24]

4.1 Schrödinger equation

The basis for quantum chemical treatment of stable atoms and molecules is the time-independent Schrödinger equation (in atomic units):

$$(5) \qquad -\frac{1}{2}\Delta\psi(x)+V(x)\psi(x)=E\psi(x), \qquad (x \in \Re^n)$$

where ψ describes the state (eigenfunction); E is the energy of the state (eigenvalue) and V is the potential under which the particle(s) are situated.[25,26,27] The measure of the set where V is discontinuous is zero. The laplacian represents the kinetic energy and V the potential energy. The eigenfunctions are required to belong to the space of quadratically integrable functions on $\Re^n$ which is denoted by $L^2(\Re^n)$. In general the wavefunctions are complex-valued functions, but in non-relativistic quantum mechanics the wave functions of stationary states are real.[26] Hence we restrict our discussion to real wave functions. Since the electrons are fermions this further restricts the eigenfunctions to the antisymmetrized subspace of L^2. The eigenfunctions are chosen so that they are normalized to unity with respect to the usual L^2 -norm. In a case of degenerate eigenvalues the corresponding eigenfunctions are chosen to be orthogonal by the normal L^2 -inner product. For an atom or a molecule the potential term is defined as:

$$(6) \qquad V(e_1,e_2,\ldots,e_k,n_1,n_2,\ldots,n_l) = -\sum_{i=1}^{k}\sum_{j=1}^{l}\frac{Z_j}{|e_i-n_j|}+\sum_{\substack{i=1\\ i<j}}^{k}\sum_{j=1}^{k}\frac{1}{|e_i-e_j|}+\sum_{\substack{i=1\\ i<j}}^{l}\sum_{j=1}^{l}\frac{Z_iZ_j}{|n_i-n_j|},$$

where $e_i \in \Re^3$ are the electron coordinates, $n_i \in \Re^3$ are the nuclear coordinates, Z_i's are the nuclear charges, and k and l denote the number of electrons and nuclei, respectively.[25,26,27] Usually the energy operator is symbolized by H (Hamiltonian), which includes both kinetic and potential terms. An important result of eqn. (5) is the variation principle which states an estimate for the smallest eigenvalue.[27] Because $L^2(\Re^n)$ is a vector space there exists a unique linear combination representation of each of its elements.[28]

4.2 Hartree-Fock self-consistent field equations

For numerical methods the dimension, 3k + 3l, makes the eqn. (5) difficult to solve directly. The discretization of the problem, i.e. the expansion in chosen basis functions, produces very large matrices or high dimensional integrals which can be handled only for light atoms and small molecules. For molecules the dimension may be dropped to 3k by making the Born-Oppenheimer approximation, where the nuclei are assumed to be stationary.[27] This also simplifies the potential term of eqn. (6) so that the nuclear contribution may be added to the eigenvalues after the eqn. (5) has been solved. Still, the dimension is too large to be applied to any practical chemical problems. The solution of eqn. (5) may be reduced to k coupled 3-dimensional differential equations by making the iterative self consistent field (SCF) Hartree-Fock (HF) approximation.[29,30,31]

Discretization of the resulting SCF HF equations may be performed by the usual basis set expansion method leading to the secular equations and the matrix eigenproblem. Grid based methods may also be applied. Examples of the grid based methods are the finite difference and the finite element methods.[32,33] Regardless of the applied method, the problem reduces to finding the eigenvalues and the corresponding eigenvectors of a generalized

matrix eigenproblem. In the case of SCF HF with MO's constructed as linear combination of AO's, the resulting matrix eigenproblem is called the Roothaan-Hall equation.[29,34,35,36]

The SCF HF treatment of the ground state will give an energy correct only to the Hartree-Fock limit, which is higher than the correct electronic energy. The method may be refined by including electron correlation effects into the calculation. Examples of these post Hartree-Fock methods are: configuration interaction (CI), Møller-Plesset perturbation (MP), and Coupled Cluster (CC).[37] Electron correlation needs to be considered when accurate energies or good quality wave functions are required.[29]

An important variable when performing calculations on radicals is the expectation value of the S^2 operator of the radical molecule. For doublet state radicals this value should be close to 0.75. However, in the spin unrestricted HF method (UHF), the values are usually higher than this. This problem is called the spin contamination and it originates from the fact that the wave function obtained by the UHF procedure is not necessarily an eigenfunction of the S^2 operator.[34,38,39] When electron correlation effects are included in the calculation, the spin contamination problem is reduced.

4.3 Semiempirical methods

The semiempirical INDO (Intermediate Neglect of Differential Overlap) and AM1 methods were applied in this work mainly for reference purposes. A detailed descriptions of these methods can be found in Refs. 40 and 41, respectively. AM1 represents one of the latest semi-empirical methods whereas INDO has been widely used by EPR spectroscopists because it is computationally feasible and it gives a correct order of magnitude for the calculated IHFCs. However, in many cases the assignment of the IHFC sign and the position by INDO gives incorrect results. A good example of this problem is the 9,10-anthraquinone anion radical (See Table 4.23 in Ref. 40). In this case the assignment of the IHFCs to α and β-positions were reversed and the sign of the β-position IHFC was wrong.

4.4 Kohn-Sham self-consistent field equations

An alternative approach for the SCF HF procedure is offered by the density functional theory (DFT). The DFT is based on the Hohenberg-Kohn theorem, which states that the ground-state energy of a many-electron system is uniquely determined by its electron density, $\rho(x)$, and that any other electron density will give higher energy.[42] A simplified proof of this statement is given by Levy.[43] Hohenberg and Kohn also concluded that the electron kinetic and electron-electron repulsion terms may be expressed as a functional of the electron density. Unfortunately the exact form of the complete functional is not known but only suggests the following partitioning of the energy functional:

$$E(\rho) = T(\rho) + U(\rho) + E_{xc}(\rho), \tag{7}$$

where the functional T describes the kinetic energy of the non-interacting electron gas, U is the classical electrostatic energy, and E_{xc} represents both the exchange and correlation energies.[44,45,46] This is the usual partitioning of the energy functional when deriving the Kohn-Sham (KS) formalism. The electron density is defined as a sum of one-electron KS orbital densities:[45,46,47]

$$\rho(x) = \sum_{i=1}^{k} |\psi_i(x)|^2 \tag{8}$$

The densities for α and β spins, ρ_α and ρ_β, may defined in similar way by including only the corresponding spin orbitals in eqn. (8). The kinetic and classical electrostatic terms can then be written as:[46]

$$T(\rho) = -\frac{1}{2}\sum_{i=1}^{k}\int_{\Re^3}\psi_i(x)\Delta\psi_i(x)dx$$

(9)
$$U(\rho) = \int_{\Re^3}\rho(x)\left(\sum_{j=1}^{l}\frac{-Z_j}{|x-n_j|}\right)dx + \frac{1}{2}\int\int_{\Re^3\Re^3}\frac{\rho(x)\rho(y)}{|x-y|}dxdy$$

Eqn. (9) assumes the Born-Oppenheimer approximation and therefore the nuclear-nuclear repulsion energy must be included when evaluating the total energy of eqn. (7). The SCF equations corresponding to eqn. (9) can be derived:

(10)
$$\left(-\frac{\Delta}{2} + \sum_{i=1}^{l}\frac{-Z_i}{|x-n_i|} + \int_{\Re^3}\frac{\rho(y)}{|x-y|}dy + \frac{\delta E_{xc}(\rho(x))}{\delta\rho(x)}\right)\psi_i(x) = \varepsilon_i\psi_i(x)$$

where the ε_i and ψ_i are the one-electron SCF KS eigenvalues and -functions and the functional derivative $\frac{\delta E_{xc}(\rho)}{\delta\rho}$ is the exchange-correlation potential corresponding to the exchange-correlation energy E_{xc}.[46] Using the linear combination of AO's a Roothaan-Hall type matrix equation may be derived in similar fashion to SCF HF theory. When a molecule or atom has unpaired electrons, the E_{xc} becomes dependent on both the electron density and the spin density. The SCF KS eigenvalues do not have the same Koopmans' theorem property as the SCF HF eigenvalues.[45] The exact form of the exchange-correlation energy E_{xc} and the corresponding potential are unknown. For example, in the local density approximation (LDA) the E_{xc} is written as:

(11)
$$E_{xc}(\rho) = -\frac{3}{2}\left(\frac{3}{4\pi}\right)^{1/3}\int_{\Re^3}\rho(x)^{4/3}dx + E_c(\rho)$$

where $E_c(\rho)$ denotes the correlation functional.[34] In this approximation it is assumed that the electron density varies slowly. Various other approximations for this functional have

been proposed.[45,46,47] These approximations include combinations of local and non-local (gradient corrected) forms. At present the hybrid functionals B3LYP and B3PW91 are the most popular functionals.[34,48,49,50,51,52] It is important to note that the SCF HF is actually a special case of SCF KS, when the exchange energy is given only by the HF exchange integral and the correlation energy is zero. Therefore the SCF KS based methods can be implemented relatively easily into the existing SCF HF computer programs. In some cases the DFT methods do not produce accurate or even qualitatively correct results, thus these methods are no substitute for the post-Hartree-Fock methods.[39]

4.5 Technical notes on calculations

The Gaussian 94 computational chemistry package was used in the theoretical calculations of this work.[53] It contains, for example, evaluation of the electronic energy by various *ab initio* and semiempirical methods, geometry optimization, and evaluation of some electronic properties based on the obtained wave function. The Gaussian 94 implementation of the SCF HF method scales as $O(N^4)$ and the SCF KS methods come very close to this, depending on the exchange-correlation term used. Most CI methods in Gaussian 94 are somewhere in the range of $O(N^5)$ and $O(N^7)$, depending also on the number of Slater determinants chosen. Here N is the number of the basis functions.[34]

Assumption of the Born-Oppenheimer approximation was standard throughout this work. The geometry of a molecule may be optimized to the energy minimum by well-known optimization procedures.[54] These methods involve calculation of the first and possibly the second derivatives of the energy with respect to the nuclear coordinates. If $|\nabla E(x)| = 0$ and the Hessian matrix at x is positive definite, then the energy E has a local minimum at x. The Hessian matrix consists of the second derivatives of energy with respect to the nuclear coordinates. It is important to test the positive definiteness of the Hessian since the energy gradient norm is zero at the energy maxima and at the saddle points too. These properties are

usually computed with the IR frequency calculations in most *ab initio* programs. Geometry restrictions may be included easily into the optimization by using penalty terms.[54]

The molecular orbitals are formed as a linear combination of suitable basis functions. Descriptions of the commonly used basis sets can be found from Ref. 34.

4.6 Calculation of isotropic hyperfine coupling constants

The isotropic hyperfine coupling constant of an organic electronic doublet state radical is related to the normalized spin density at nucleus *N* by the relation:[29]

(12) $$a(N) = \frac{2}{3} g_N \beta_N \mu_0 D(r_N)$$

where a is the IHFC value at nucleus N (T), g_N is the nuclear g-value, β_N is the nuclear magneton, μ_0 is the vacuum permeability, and $D(r_N) = \rho_\alpha - \rho_\beta$ is the normalized spin density at the nucleus *N*.

Because the electron-nuclear potential term of eqn. (5) is discontinuous at the nuclei, the resulting wave function is not expected to be numerically stable at that point, and therefore the IHFC is not an easy property to calculate. Also most *ab initio* programs use the Gaussian-type orbitals which do not fulfill the cusp condition at the nuclei. Various approaches have been suggested to overcome these problems.[55,56] Before the DFT methods became widely used, the calculation of IHFCs required a large, well balanced basis set combined with CI calculations with single and double substitutions included. These CI calculations were only applicable to relatively small radicals. For example the methyl radical has been studied with the CI methods.[57] The new E_{xc} functionals of the KS method have recently been shown to be able to predict IHFCs for organic radicals.[58,59] A good recent review of the calculation of IHFCs by CI and DFT methods has been given by Lunell *et al.*[60] Since the computational requirement of the DFT is often less than that of CI, calculations on larger organic radicals, such as alkyl substituted 9,10-anthraquinone anion radicals, have

used DFT methods. On the basis of various studies the B3LYP functional with the polarized split valence 6-31G* type basis set has proven to be a good level of approximation when calculating the IHFCs.[58,59]

To get an impression of the accuracy of the applied B3LYP/6-31G* method, the calculated and experimental IHFCs of a series of small radicals are presented in Table 1. Some differences between the experimental and calculated results may arise from the static geometry applied in the calculations and the possible matrix effects present in the experiments. For protons the calculated IHFCs are usually within 10 % of the experimental results and the expectation values of the S^2 operator are very close to the correct value of 0.75 in all the cases considered.

Table 1. Theoretical (optimized by B3LYP/6-31G*) and experimental IHFCs for some small radicals. The references are given for the experimental data whereas the calculated values were produced during this work. The IHFCs are expressed in units of mT.

Compoun	State	Nucl.	$a_{1,calc}$	$a_{1,expt}$	Nucl.	$a_{2,calc}$	$a_{2,expt}$	Ref.
H_2O^+	Doublet	^1H	-2.51	2.61	^{17}O	-3.09	2.97	61
OH	Doublet	^1H	-2.43	2.28 - 2.62	^{17}O	-1.82	2.28 - 2.62	62,63,64
CN	Doublet	^{13}C	+18.3	21.0	^{14}N	-0.63	0.45	61
CH_3	Doublet	^1H	-2.53	2.47	^{13}C	+4.42	2.70	65
CH	Doublet	^1H	-1.82	2.06	^{13}C	+1.67	1.68	66, 67
C_2H_5	Doublet	^1H	-2.41	2.24	^1H	+2.64	2.69	68 (*)
NO	Doublet	^{14}N	+0.64	0.79	^{17}O	-1.13	--	69

(*) Methyl protons were averaged in the IHFC calculation.

The calculated IHFCs are not heavily sensitive to the choice of basis set but the required accuracy is usually reached at the 6-31G* basis set level. For example, in the case of CH radical even the STO-3G basis set is sufficient to reproduce the experimental observations.

4.7 Zero-point and temperature corrections to isotropic hyperfine coupling constants

The zero-point and temperature averaged effects of molecular vibration on the observed IHFCs have been considered recently by Barone *et al.*[70] As an example of their method, the planar methyl radical is briefly considered here. The vibrational effect in this molecule is caused by the out-of-plane movement of the carbon atom. This movement is taking place at the bottom of a one dimensional potential well. The potential energy curve and the IHFC dependence curve were calculated by issuing constraints to the methyl radical geometry and performing constrained geometry optimizations. The quantized nuclear energies and states were obtained by solving the one-dimensional Schrödinger equation for vibration. The energy levels obtained were then weighted by assuming the Boltzmann distribution among the states. Finally, the temperature averaged IHFC values were calculated. This treatment yielded a very good agreement with the observed ^{13}C IHFC values. Because good results were obtained, it is reasonable to extend this treatment to model the internal rotation in hydroquinone-like cation radicals as well.

The internal rotation of some groups with respect to each other may be described by the one-dimensional torsional Schrödinger equation (Mathieu equation) for the rotating groups:

$$-F\frac{\partial^2\psi(\alpha)}{\partial\alpha^2} + V(\alpha) = E\psi(\alpha), \tag{13}$$

where the periodic boundary conditions to ψ apply on interval $[0,2\pi]$.[71,72] V describes the potential under which the groups rotate, $F = h^2/(8\pi^2 I)$, I is the reduced moment of inertia of the rotating groups, and ψ and E are the torsional nuclear eigenfunctions and -values. Depending on the form of the potential V, some approximate solutions are possible to eqn.

(13). For example, for an infinitely high rotation barrier the harmonic oscillator model may be used. To obtain a general solution, the problem must be solved numerically. The problem may be solved easily by applying the finite difference approximation to eqn. (13) and computing the eigenvalues and eigenvectors of the resulting matrix.[73] Let us denote the operator, which describes the torsional dependence of the IHFC, by $A(\alpha)$. Then the zero point and temperature averaged IHFC at temperature T may be expressed as:

$$a_{eff}(T) = \frac{\sum_i e^{-E_i/RT} \langle \psi_i | A | \psi_i \rangle}{\sum_i e^{-E_i/RT}}, \tag{14}$$

where R is the gas constant.[70,72] This result may be readily derived using the density matrix formalism by noting that the density matrix for thermal equilibrium is:

$$\sigma = \frac{e^{-H/RT}}{Tr(e^{-H/RT})} \tag{15}$$

where H is the torsional nuclear Hamiltonian of eqn. (13).[8] The potential term V may usually be approximated in the case of a symmetric rotation barrier with the first Fourier term:

$$V(\alpha) = \frac{V_0}{2}(1 - \cos(n\alpha)) \tag{16}$$

where V_0 is the height of the potential barrier and n is the number of minima on the potential curve.[71] In many cases the IHFC operator $A(\alpha)$ has been found to follow a very similar relation:

(17) $$A(\alpha) = a_p + \frac{a_o - a_p}{2}(1 - \cos(n\alpha))$$

where a_p and a_0 are the IHFC values at the minimum of the potential curve and at the maximum, respectively.[72] The quantity $(a_0\text{-}a_p)/2$ is called the IHFC barrier height and is usually obtained from the theoretical calculations. Since the term F includes the reduced moment of inertia of the rotating groups, isotope effects may be studied. Moments of inertia obtained from the theoretically calculated rigid geometries were applied in this work. Quantum tunneling effects may also be observed, if the rotation barrier height and width are suitable. The tunneling phenomenon can easily be identified by inspecting the nuclear wave functions. No such effect was observed in this work because the rotation barrier heights and widths were not suitable.

The outlined method can be applied in two ways: by calculating the zero-point and the temperature dependent correction for theoretically derived IHFCs or by estimating the values of given variables from the experimental IHFC vs. temperature data. An example of the first case is presented in paper 4 and of the second case in paper 5. For analyzing the experimental data in Paper 5, it was neccessary to include a least squares fitting routine over the temperature dependence model program of Paper 4. Both programs are available upon request.

5. SUMMARY AND CONCLUSIONS

5.1 Comparison of spin density calculation methods for various alkyl-substituted 9,10-anthraquinone anion radicals in the solution phase

The objective of the study was to test various computational methods for calculating the isotropic hyperfine coupling constants in alkyl-substituted 9,10-anthraquinones (AQ). Currently only deuteration can be considered as a reliable method for assigning the hyperfine couplings to specific magnetic nuclei. The deuteration process is usually a tedious task and sometimes impossible. If a reliable computational method is found then the assignation can be made a routine task.

Anion radicals of 2-methylAQ, 2-ethylAQ, 2-*tert*-butylAQ, and 2,3-dimethylAQ were generated in various solvents. EPR and ENDOR spectra of the compounds were measured and the spectra were analyzed using the iterative simulation fitting procedure. The obtained isotropic hyperfine coupling constants were compared with the calculated values obtained from INDO, AM1/CI, and B3PW91 methods. AM1/CI and B3PW91 methods were the best methods considered in the study but still the results were not very accurate. To obtain better accuracy solvent effects have to be considered.

5.2 EPR, ENDOR and TRIPLE resonance of amino-substituted 9,10-anthraquinone radicals and the rotation of the amino groups in the solution phase

The aim of the study was to gain information about the existence of a hydrogen bond between the amino group protons at positions 1, 4, 5, and 8 and the quinone oxygens at positions 9 and 10. The measured isotropic hyperfine coupling constants are also valuable as reference data.

Anion radicals of 1-aminoAQ, 2-aminoAQ, 1,4-aminoAQ, 1,5-diaminoAQ, and 2,6-diaminoAQ were generated in various solvents. The isotropic hyperfine coupling constants were obtained from the EPR and ENDOR data using the iterative simulation fitting procedure. The observation of non-equivalent amino protons in 1,5-diaminoAQ anion radical indicated that the amino groups can only be rotating slower than can be distinguished by the EPR experiments. The theoretically calculated amino group rotation barrier for positions 1, 4, 5, and 8 were considerably higher than for positions 2, 3, 6, and 7. These results show the existence of the hydrogen bonding between the α-position amino group proton and the quinone oxygen.

5.3 Molecular orbital study of conformational isomers and rotational barriers of methyl-substituted hydroquinone cation radicals

The aim of this study was to validate various theoretical methods by reference to the experimental data and to obtain information about the cis-trans isomerization of the methyl substituted hydroquinone cation radicals.

The minimum and the torsional transition state geometries and energies were computed by using the high accuracy density functional methods yielding the rotation barrier height and the energy difference between the cis and trans isomers. The energy minima were located for methyl-hydroquinone, 2,3-dimethyl-hydroquinone, 2,5-dimethyl-hydroquinone, 2,6-dimethyl-hydroquinone, and trimethyl-hydroquinone cation radicals. The obtained results for rotation barrier heights and the number of isomers were in reasonable agreement with the earlier experimental results. The rather high hydroxyl group rotation barrier height is caused by a partial double bond character of the C-O bond.

5.4 Molecular orbital study of the isotropic hyperfine coupling constants of hydroquinone and tetramethylhydroquinone cation radicals

The objective of the study was to calculate the zero-point and temperature dependent corrections to the hydroxyl proton, ring proton, and ^{17}O isotropic hyperfine coupling constants in the hydroquinone and tetramethylhydroquinone cation radicals.

The applied computational model yielded the temperature dependence of the isotropic hyperfine coupling constants in agreement with earlier experimental observations. The zero-point and temperature dependent corrections are essential in order to reproduce the experimental results.

5.5 Temperature dependence of the isotropic hyperfine coupling constants in 1,4-hydroquinone and 1,4-dihydroxynaphthalene cation radicals

The aim of this paper was to obtain experimental values for the hydroxyl group rotation barriers, information on the isotope effect on the hydroxyl group rotation, and a demonstration of the accuracy of the modern spectrum analysis methods.

The isotropic hyperfine coupling constants were measured for both cation radicals on the temperature range of 150 - 300 K using various solvents. The obtained hydroxyl group temperature dependence data yielded new values for the rotation barrier heights for both compounds. These new values are somewhat higher than determined in the earlier studies. Deuteration of the hydroxyl group proton resulted in lowered torsional zero-point energy. Accurate computer simulations of the EPR spectra revealed that the temperature dependence of the hydroxyl proton IHFC is not linear. This non-linearity was predicted theoretically in paper 4.

6. THE AUTHOR'S CONTRIBUTION ON RESEARCH PAPERS

Paper 1: I have undertaken some of the experimental measurements, simulated the EPR spectra, performed all the *ab initio* calculations, and written the paper.

Paper 2: I have performed *ca.* half of the experimental measurements, simulated the EPR spectra, performed all the *ab initio* calculations, and written the paper.

Paper 3: I have made some of the *ab initio* calculations and written the paper.

Paper 4: I have performed all the *ab initio* calculations, written all the required computer programs, and written the paper.

Paper 5: I have prepared the vacuum samples, made all the measurements, written all the required computer programs, and written the paper.

7. REFERENCES

1. W. Gerlach and O. Stern, *Z. Phys.* **8**, 110 (1921).
2. W. Gerlach and O. Stern, *Z. Phys.* **9**, 349 (1922).
3. W. Gerlach and O. Stern, *Z. Phys.* **9**, 353 (1922).
4. G. Breit and I. I. Rabi, *Phys. Rev.* **38**, 2082 (1931).
5. I. I. Rabi, J. R. Zacharias, S. Millman and P. Kusch, *Phys. Rev.* **53**, 318 (1938).
6. E. Zavoisky, *J. Phys. U.S.S.R.* **9**, 211, 245 (1945).
7. J. A. Weil, J. R. Bolton and J. E. Wertz, *Electron Paramagnetic Resonance: Elementary Theory and Practical Applications*, Wiley-Interscience (1994).
8. N. M. Atherton, *Principles of Electron Spin Resonance*, Prentice Hall (1993).
9. A. Carrington and A. D. McLachlan, *Introduction to Magnetic Resonance*, Harper & Row and John Waterhill (1967).
10. H. M. McConnell, *J. Chem. Phys.* **28**, 430 (1958).
11. J. Eloranta, ftp://endor.chem.jyu.fi/pub.
12. J. R. Norris, Jr., *Chem. Phys. Lett.* **1**, 333 (1967).
13. J. Heinzer, *Mol. Phys.* **22**, 167 (1971).
14. J. Kevan and L. D. Kispert, *Electron Spin Double Resonance Spectroscopy*, John Wiley & Sons (1976).
15. H. Kurreck, B. Kirste and W. Lubitz, *Electron Nuclear Double Resonance Spectroscopy of Radicals in Solution*, VCH Publishers (1988).
16. B. Kirste, *J. Magn. Reson.* **73**, 213 (1987).
17. J. A. Nedler and R. Mead, *Comput. J.* **7**, 308 (1965).
18. A. L. J. Beckwith and S. Brumby, *J. Magn. Reson.* **73**, 252 (1987).
19. Designed and built by M. Vuolle, H. van Willigen, R. Kauppinen and E. Järvinen.
20. G. Cauquis, *Bull. Chim. Soc. Fr.*, 459 (1966).
21. G. Cauquis, *Bull. Chim. Soc. Fr.*, 1618 (1968).
22. K. Kratochvil and M. Nepras, *Collect. Czech. Chem. Commun.* **37**, 1533 (1972).
23. R. Mäkelä, *Dissertation*, University of Jyväskylä (1990).

24. M. Head-Gordon, *J. Phys. Chem.* **100**, 13213 (1996).

25. M. Alonso and E. J. Finn, *University Physics, Volume III: Quantum and Statistical Physics*, Addison-Wesley Publishing Company (1968).

26. L. D. Landau and E. M. Lifschitz, *Quantum Mechanics, Non-relativistic Theory (3rd edition)*, Pergamon Press, Oxford (1977).

27. P. W. Atkins, *Molecular Quantum Mechanics (2nd edition)*, Oxford University Press (1983).

28. A. Friedman, *Foundations of Modern Analysis*, Dover Publications (1982).

29. R. McWeeny, *Methods of Molecular Quantum Mechanics (2nd edition)*, Academic Press (1992).

30. W. G. Richards and J. A. Horsley, *Ab Initio Molecular Orbital Calculations for Chemists*, Oxford Clarendon Press (1970).

31. I. G. Csizmadia, *Theory and Practice of MO Calculations on Organic Molecules*, Elsevier Scientific Publishing Company (1976).

32. J. Kobus, L. Laaksonen and D. Sundholm, *Comput. Phys. Commun.* **98**, 464 (1996).

33. M. Krizek and P. Neittaanmäki, *Finite Element Approximation of Variational Problems and Applications*, Longman Scientific & Technical (1990).

34. J. B. Foresman and Æleen Frisch, *Exploring Chemistry with Electronic Structure Methods (2nd edition)*, Gaussian, Inc. (1996).

35. C. C. J. Roothaan, *Rev. Mod. Phys.* **23**, 69 (1951).

36. G. G. Hall, *Proc. Royal Soc. (London) A* **205**, 541 (1951).

37. K. Raghavachari and J. B. Anderson, *J. Phys. Chem.* **100**, 12960 (1996).

38. J. Wang, A. D. Becke and V. H. Smith, Jr., *J. Chem. Phys.* **102**, 3477 (1995).

39. M. W. Wong and L. Radom, *J. Phys. Chem.* **99**, 8582 (1995).

40. J. A. Pople and D. L.Beveridge, *Approximate Molecular Orbital Theory*, McGraw-Hill Book Company (1970).

41. M. J. S. Dewar, E. G. Zoebisch and E. F. Healy, *J. Am. Chem. Soc.* **107**, 3902 (1985).

42. P. Hohenberg and W. Kohn, *Phys. Rev. B* **136**, 864 (1964).

43. M. Levy, *Proc. Natl. Acad. Sci.* **76**, 6062 (1979).

44. W. Kohn and L. J. Sham, *Phys. Rev. A* **140**, 1133 (1965).

45. R. O. Jones and O. Gunnarssson, *Rev. Mod. Phys.* **61**, 689 (1989).

46. Ed. J. Seminario, *Modern Density Functional Theory: A Tool for Chemistry*, Elsevier Science B. V. (1995).

47. W. Kohn, A. D. Becke and R. G. Parr, *J. Phys. Chem.* **100**, 12974 (1996).

48. A. D. Becke, *J. Chem. Phys.* **98**, 5648 (1993).

49. S. H. Vosko, L. Wilk and M. Nusair, *Can. J. Phys.* **58**, 1200 (1980).

50. C. Lee, W. Yang and R. G. Parr, *Phys. Rev. B* **37**, 785 (1988).

51. B. Miehlich, A. Savin, H. Stoll and H. Preuss, *Chem. Phys. Lett.* **157**, 200 (1989).

52. J. P. Perdew and Y. Wang, *Phys. Rev. B* **45**, 13244 (1992).

53. M. J. Frisch, G. W. Trucks, H. B. Schlegel, P. M. W. Gill, B. G. Johnson, M. A. Robb, J. R. Cheeseman, T. A. Keith, G. A. Petersson, J. A. Montgomery, K. Raghavachari, M. A. Al-Laham, V. G. Zakrzewski, J. V. Ortiz, J. B. Foresman, J. Cioslowski, B. B. Stefanov, A. Nanayakkara, M. Challacombe, C. Y. Peng, P. Y. Ayala, W. Chen, M. W. Wong, J. L. Andres, E. S. Replogle, R. Gomperts, R. L. Martin, D. J. Fox, J. S. Binkley, D. J. Defrees, J. Baker, J. P. Stewart, M. Head-Gordon, C. Gonzalez and J. A. Pople, *Gaussian 94 Revision B.3*, Gaussian, Inc., Pittsburgh, PA (1995).

54. R, Fletcher, *Practical Methods of Optimization* (*2nd edition*), John Wiley & Sons (1987).

55. D. M. Chipman, *Theor. Chim. Acta* **82**, 93 (1992).

56. V. A. Rassolov and D. M. Chipman, *J. Chem. Phys.* **105**, 1470 (1996).

57. D. M. Chipman, *J. Chem. Phys.* **78**, 3112 (1983).

58. V. Barone, *Chem. Phys. Lett.* **262**, 201 (1996).

59. P. J. O'Malley and S. J. Collins, *Chem. Phys. Lett.* **259**, 296 (1996).

60. B. Engels, L. A. Eriksson and S. Lunell, *Adv. Quantum Chem.* **20**, 297 (1996).

61. L. B. Knight, Jr. and J. Steadman, *J. Chem. Phys.* **78**, 5940 (1983).

62. W. Weltner, Jr., *Magnetic Atoms and Molecules*, van Nostrand, NY (1983).

63. K. R. Leopold, K. M. Evenson, E. R. Comben and J. M. Brown, *J. Mol. Spectrosc.* **122**, 440 (1987).

64. A. Carrington and N. J. D. Lucas, *Proc. R. Soc. London Ser. A.* **314**, 576 (1970).

65. R. W. Fessenden, *J. Phys. Chem.* **71**, 74 (1967).

66. T. C. Steimle, D. R. Woodward and J. M. Brown, *J. Chem. Phys.* **85**, 1276 (1986).

67. C. R. Brazier and J. M. Brown, *Can. J. Phys.* **62**, 1563 (1984).

68. R. W. Fessenden and R. H. Schuler, *J. Chem. Phys.* **39**, 2147 (1963).

69. W. L. Meerts and A. Dymanus, *J. Mol. Spectrosc.* **44**, 320 (1972).

70. V. Barone, A. Grand, C. Minichino and R. Subra, *J. Chem. Phys.* **99**, 6787 (1993).

71. W. J. Orville-Thomas, in *Internal Rotation in Molecules*, John Wiley & Sons (1974).

72. N. L. Bauld, J. D. McDermed, C. E. Hudson, Y. S. Rim, J. Zoeller, Jr., R. D. Gordon and J. S. Hyde, *J. Am. Chem. Soc.* **91**, 6666 (1969).

73. F. Scheid, *Theory and Problems of Numerical Analysis*, McGraw-Hill Book Company (1986).

ORIGINAL PUBLICATIONS

PAPER 1

Magn. Reson. Chem. **34**, 898-902 (1996).

https://doi.org/10.1002/(SICI)1097-458X(199611)34:11<898::AID-OMR985>3.0.CO;2-R

PAPER 2

Magn. Reson. Chem. **34**, 903-907 (1996).

https://doi.org/10.1002/(SICI)1097-458X(199611)34:11<903::AID-OMR986>3.0.CO;2-8

PAPER 3

J. Mol. Struct. (*THEOCHEM*), in press (1997).

https://doi.org/10.1016/S0166-1280(97)00152-8

PAPER 4

J. Chem. Soc., Faraday Trans. **93**, 3313-3317 (1997).

https://doi.org/10.1039/A701894K

PAPER 5

Magn. Reson. Chem., in press (1997).

https://doi.org/10.1002/(SICI)1097-458X(199802)36:2<98::AID-OMR228>3.0.CO;2-Q